Electrochemical Synthesis of $LiTiO_2$ and $LiTi_2O_4$ in Molten LiCl

Kai Jiang,[†,‡] Xiaohong Hu,[†] Huijiao Sun,[†] Dihua Wang,[†] Xianbo Jin,[†] Yaoyao Ren,[‡] and George Z. Chen*[,†,§]

College of Chemistry and Molecular Science, and Centre for Electron Microscopy, Wuhan University, Wuhan, 430072, People's Republic of China, and School of Chemical, Environmental and Mining Engineering, University of Nottingham, University Park, Nottingham NG7 2RD, U.K.

Received April 7, 2004. Revised Manuscript Received August 4, 2004

The rock salt-type $LiTiO_2$ and spinel-type $LiTi_2O_4$ were synthesized with accurate control of stoichiometry by electrochemical insertion of Li^+ into solid TiO_2 (anatase) in molten LiCl. The behavior of Li^+ insertion was investigated by cyclic voltammetry using a "TiO_2 powder modified molybdenum electrode". The results indicate two Li^+ insertion reactions at two different potentials for the formation of $LiTiO_2$ and $LiTi_2O_4$, respectively, as confirmed by ICP, XRD, and TEM analyses.

1. Introduction

The ternary Li−Ti−O system consists of various stoichiometric and nonstoichiometric compounds, of which many exhibit useful and/or interesting functionalities from both practical and academic points of view.[1−10] For example, as the breeding material in the blanket of a nuclear reactor, the monoclinic Li_2TiO_3 is effective in producing tritium atom by lithium transmutation.[11] The spinel-type $LiTi_2O_4$ exhibits superconductivity up to 13 K, which has attracted considerable attention following the discovery by Johnston et al. in 1976.[12,13] This spinel compound also shows a high reversibility for lithium insertion as the negative electrode in lithium ion batteries with, for example, $LiCoO_2$ or $LiMnO_2$ as the positive electrode.[14,15] Such a battery is advantageous in that lithium metal, which is expensive to produce and risky to handle, is eliminated in both the manufacturing and the application processes. The rock salt-type $LiTiO_2$ is believed to be conducting and also the end member of a series of compounds, Li_xTiO_2 ($0 \le x \le 1$), resulting from lithium insertion into TiO_2.[16] Although its existence has been well recognized theoretically[16−19] and extrapolated experimentally,[19−21] $LiTiO_2$ (or the metastable cubic $Li_2Ti_2O_4$ as originally reported which could be converted to the rock salt $LiTiO_2$ upon heating to 600 °C) was only isolated in a few cases by chemical synthesis,[3,22,23] but electrochemical means have not yet been used to produce this compound.

In all of the reported studies, the Li−Ti−O compounds were usually prepared by sintering the powder samples (Li_2CO_3, Ti_2O_3, TiO_2, etc.) through several consecutive processes at elevated temperatures (500−1000 °C)[12,19,24−28] or by the reaction of lithium metal

* To whom correspondence should be addressed. Telephone: +86-27-87210319/+44-115-9514171. Fax: +86-27-87210319/+44-115-9514115. E-mail: george.chen@nottingham.ac.uk.
† College of Chemistry and Molecular Science, Wuhan University.
‡ Centre for Electron Microscopy, Wuhan University.
§ University of Nottingham.

(1) Strobel, P.; Cras, F. L.; Anne, M. *J. Solid State Chem.* **1996**, *124*, 83.
(2) Lambert, P. M.; Harrison, M. R.; Edwards, P. P. *J. Solid State Chem.* **1988**, *75*, 332.
(3) Cava, R. J.; Murphy, D. W.; Zahurak, S.; Santoro, A.; Roth, R. S. *J. Solid State Chem.* **1984**, *53*, 64.
(4) Liao, Y. C.; Xu, F.; Wang, M. J.; Wu, C.; Wu, M. K. *J. Low Temp. Phys.* **2003**, *131*, 781.
(5) Kavan, L.; Fattakhova, D.; Krtil, P. *J. Electrochem. Soc.* **1999**, *146*, 1375.
(6) Gover, R. K. B.; Tolchard, J. R.; Tukamoto, H.; Murai, T.; Irvine, J. T. S. *J. Electrochem. Soc.* **1999**, *146*, 4348.
(7) Kuhn, A.; Amandi, R.; Garcia-Alvarado, F. *J. Power Sources* **2001**, *92*, 221.
(8) Ebina, T.; Iwasaki, T.; Onodera, Y.; Hayashi, H.; Nagase, T.; Chatterjee, A.; Chiba, K. *J. Power Sources* **1999**, *81−82*, 393.
(9) Koudriachova, M. V.; Harrison, N. M.; Leeuw, S. W. de. *Solid State Ionics* **2002**, *152−153*, 189.
(10) Wagemaker, M.; Kearly, G. J.; Well, A. A. van.; Mutka, H.; Mulder, F. M. *J. Am. Chem. Soc.* **2003**, *125*, 840.
(11) Kleykamp, H. *Fusion Eng. Des.* **2002**, *61*, 361.
(12) Johnston, D. C. *J. Low Temp. Phys.* **1976**, *25*, 145.
(13) Chen, C.; Spears, M.; Wondre, F.; Ryan, J. *J. Cryst. Growth* **2003**, *250*, 139.
(14) Krtil, P.; Fattakhova, D. *J. Electrochem. Soc.* **2001**, *148*, A1045.
(15) Manickam, M.; Takata, M. *J. Power Sources* **2003**, *114*, 298.
(16) Mackrodt, W. C. *J. Solid State Chem.* **1999**, *142*, 428.
(17) Benco, L.; Barras, J. L.; Daul, C. A.; Deiss, E. *Inorg. Chem.* **1999**, *38*, 20.
(18) Koudriachova, M. V.; Harrison, V. M.; Leeuw, S. W. de. *Phys. Rev. Lett.* **2001**, *86*, 1275.
(19) Lecerf, A. *Ann. Chim.* **1962**, *7*, 519.
(20) Shirane, G.; Pickarty, S. J.; Newnham, R. *J. Phys. Chem. Solids* **1960**, *12*, 155.
(21) Koudriachova, M. V.; Leeuw, S. W. de.; Harrison, N. M. *Chem. Phys. Lett.* **2003**, *371*, 150.
(22) Murphy, D. W.; Greenblatt, M.; Zahurak, S. M.; Cava, R. J.; Waszczak, J. V.; Hull, G. W.; Hutton, R. S. *Rev. Chim. Miner.* **1982**, *19*, 441.
(23) Murphy, D. W.; Cava, R. J.; Zahurak, S. M.; Santoro, A. *Solid State Ionics* **1983**, *9−10*, 413.
(24) Deschanvres, A.; Raveau, B.; Sekkal, Z. *Mater. Res. Bull.* **1971**, *6*, 699.
(25) Johnston, D. C.; Prakash, H.; Zachariasen, W. H.; Viswanathan, R. *Mater. Res. Bull.* **1973**, *8*, 777.
(26) Harrison, M. R.; Edwanrds, P. P.; Goodenough, J. B. *J. Solid State Chem.* **1984**, *54*, 136.
(27) Ueda, Y.; Tanaka, T.; Kosuge, K. *J. Solid State Chem.* **1988**, *77*, 401.
(28) Xu, F.; Liao, Y. C.; Wang, M. J.; Wu, C. T.; Chiu, K. F.; Wu, M. K. *J. Low Temp. Phys.* **2003**, *131*, 569.

10.1021/cm0494148 CCC: $27.50
Published on Web 09/23/2004

with titanium oxides in a sealed steel vessel above 1100 °C for several decades of hours.[29,30] Multistep hydrothermal synthesis by reacting titanium oxides with LiOH in water at relatively low temperatures (130−200 °C) followed by postsynthesis annealing up to 500 °C was also reported.[31] More recent techniques involved reactions between organic lithium and titanium compounds in organic solvents at room temperature, followed by annealing to 500−800 °C under nitrogen for more than 10 h.[14,22] Particularly, the compound $Li_2Ti_2O_4$ was obtained by reacting the $LiTi_2O_4$ spinel with *n*-BuLi.[3,23] However, the challenge is that, in many of these thermochemical processes, it is difficult to control the stoichiometry of, or to avoid the formation of, multiple phases in the product. It should be mentioned that organic lithiation agents, such as *n*-BuLi, are at present mainly synthesized from, for example, alkylhalides and lithium metal, and the latter is industrially produced by electrolysis of molten LiCl (mp = 610 °C).

Alternatively, spinel-type $LiTi_2O_4$ crystals were grown in a molten salt bath containing TiO_2, $LiBO_2$, $NaBO_2$, and NaF[32] or TiO_2, Li_2CO_3, LiF, and $Na_2B_4O_7$[13] with the assistance of electrolysis. In these processes, the cathodic reduction of Ti(IV) to Ti(III) was believed to play an important role for the formation of $LiTi_2O_4$. In comparison with the thermochemical routes, the electrochemical method provides not only a better control of the product stoichiometry but also an additional driving force for crystal growth. Nonetheless, it should be mentioned that only the electrolytic growth of $LiTi_2O_4$ crystals from the molten media was reported in the literature.

This Article reports a simple, fast, and controllable route for the electrochemical synthesis of single phase $LiTiO_2$ and $LiTi_2O_4$ from solid TiO_2 in molten LiCl. This route proceeds by making the TiO_2 powder into a cathode which is then electrolyzed in the solid state in the molten salt under mild conditions. As is shown below, this electrochemical route is highly efficient and offers a product at low cost with controlled stoichiometry and hence functionality.

2. Experimental Section

2.1. Electrochemical Synthesis. The TiO_2 powder (particle size: 100−500 nm, Tianjin Kemi'ou, China) was manually pressed into small pellets (diameter, 2.0 cm; thickness, ~0.2 cm). After the pellets were sintered at 1000 °C for 2 h, the porosity of the pellets was estimated to be between 40% and 50% on the basis of the mass and volume of the pellet, and the density of anatase. Several pellets were pressed and sandwiched between two porous nickel foils and attached onto a steel wire. This assembly was used as a cathode in constant voltage (1.2−3.2 V) electrolysis with a graphite crucible anode (inner diameter, 5.0 cm; height, 20 cm) in molten LiCl at 700 °C. The electrolytic cell was sealed in a stainless steel retort that was continuously purged with an argon flow. The effluent gases that contained chlorine from the anodic reaction were filtered through a concentrated NaOH solution before escaping to a fume hood.

To remove moisture and some other redox-active impurities from the molten salt, pre-electrolysis of the molten LiCl at 2.5 V was carried out between the graphite crucible anode and the assembled cathode without loading TiO_2. The pre-electrolysis was terminated when the current reached a low and stable current, that is, the residual or background current which is commonplace in molten salt electrolysis.[33,34] The causes for the residual current are not fully understood, but are likely related with impurities of multivalent elements that can undergo electron-transfer reactions at and transport between the anode and cathode, and more importantly conducting electrons through the electrolyte via a redox change assisted hopping mechanism.[33] An important feature of this electron conduction related residual current is that it increases with an increase in the applied cell voltage,[34] which was indeed observed in this work.

When the cathode assembly was loaded with TiO_2, the electrolysis was terminated after the recorded current decreased to the predetermined residual value. The cathode was removed from the molten salt, cooled in argon, and then washed with water in air or with acetone in an argon-filled glovebox to dissolve the salt that solidified on the exterior of the assembled cathode. After being separated from the porous nickel foils, the electrolyzed pellets were manually ground into powder with mortar and pestle, further washed with water or acetone, and dried at about 120 °C in air or in a desiccator under vacuum at room temperature before further analysis. All other chemicals were of the AnarlaR grade or equivalent and were used as received.

2.2. Cyclic Voltammetry. A "TiO_2 powder modified molybdenum electrode" was used for recording cyclic voltammograms (CVs) in molten LiCl and was fabricated as follow. A molybdenum wire (diameter, 0.2 cm; length, ~60 cm) was polished to remove the surface dirt. A pair of small and shallow notches were made at the middle of the wire using a pair of pliers. The wire was then subjected to repeated bending until the wire was broken due to work hardening. Such broken wires had an end with a fresh and significantly rough surface. The rough end of the wire was then pressed manually into a pre-heat-treated (1000 °C in air for 2 h) TiO_2 powder placed on a hard substrate, after which the pits and troughs of the rough end were filled with micrometer and submicrometer particles of the powder. After wiping the sidewall of the wire with tissue paper without touching the end, we inserted the TiO_2 powder modified molybdenum electrode into the electrolyte for recording CVs. About 40 g of LiCl powder was filled into a small graphite crucible (inner diameter, 1.8 cm; height, 25 cm), which also functioned as the counter electrode. A platinum wire was used as the pseudo-reference electrode. This three-electrode cell was sealed in a quartz tube, which was placed in a furnace and heated to 700 °C. During voltammetric experiments, argon was continuously fluxed through the quartz tube. Cyclic volta-

(29) Akimoto, J.; Gotoh, Y.; Kawaguchi, K.; Oosawa, Y. *J. Solid State Chem*. **1992**, *96*, 446.
(30) Akimoto, J.; Gotoh, Y.; Sohma, M.; Kawaguchi, K.; Oosawa, Y. *J. Solid State Chem*. **1994**, *110*, 150.
(31) Fattakhova, D.; Krtil, P. *J. Electrochem. Soc*. **2002**, *149*, A1224.
(32) Durmeyer, O.; Kappler, T. P.; Derory, A.; Drillon, M.; Capponi, J. *J. Solid State Commun*. **1990**, *74*, 621.
(33) Stohr, U.; Freyland, W. *Phys. Chem. Chem. Phys*. **1999**, *1*.
(34) Chen, G. Z.; Fray, D. J. *J. Appl. Chem*. **2001**, *31*, 155.

mmetry was performed on the EG&G M263A potentiostat/galvanostat (Princeton Applied Research, USA) with potentials ranging from 0.7 to −2.1 V.

2.3. Spectroscopic Analyses. The X-ray diffraction (XRD) patterns of the electrolytic Li−Ti−O products were obtained on the Shimadzu XRD 6000 diffractometer with Cu Kα_1 radiation (λ = 1.5405 Å) at 40 kV and 50 mA, at a scan rate of (2θ) 4 deg/min. Samples were also sent to the Materials Test and Inspection Research Institute of Wuhan Iron and Steel (Group) Corp. (Wuhan, China) for elemental analysis, particularly the contents of titanium and lithium, using inductively coupled plasma (ICP) with atomic emission spectroscopy (ICP-AES, model IRIS, TJA, USA). The JEM-2010 transmission electron microscope was used at 200 kV to take the bright field micrographs and the electron diffraction patterns.

3. Results and Discussion

3.1. Constant Voltage Electrolysis. Different voltages ranging from 1.2 to 3.2 V were applied in the electrolysis of the porous TiO_2 pellets, which were sandwiched between two porous nickel foils, in molten LiCl. Figure 1a shows a typical current−time plot recorded at 3.2 V (the total weight of the pellets was 3.48 g). It can be seen that the current is very high (>4 A) in the first 15 min of electrolysis, and then falls rapidly to a low value (<500 mA). Afterward, the current continues to decrease very slowly until a stable level of about 250 mA that is comparable with the predetermined residual current (which decreases with a lowering of the applied cell voltage). By subtracting the residual current as shown in Figure 1, the charge used for the insertion reaction was estimated to be about 1190 mAh, equivalent to 0.444 mol of electrons. This number can be compared to the number of moles of TiO_2 on the cathode, which was 0.435 mol. These results agree very well with the following Li^+ insertion reaction:

$$TiO_2 + Li^+ + e \rightarrow LiTiO_2 \quad (1)$$

When changing the voltage between 3.2 and 2.0 V, the 1:1 charge−TiO_2 correlation remained unchanged, suggesting that the electrolysis products at the cathode were also $LiTiO_2$.

However, upon further decreasing the voltage to below 1.8 V, different charge−TiO_2 correlations were observed. Figure 1b displays the current−time plot recorded at 1.8 V (the weight of the pellets was 2.98 g). After the residual current was subtracted, the total charge passed was about 510 mAh, indicating approximately a 1:2 correlation between the numbers of moles of electrons and TiO_2. This correlation is in accordance with the following Li^+ insertion reaction.

$$2TiO_2 + Li^+ + e \rightarrow LiTi_2O_4 \quad (2)$$

The charge passed during electrolysis at 1.6 V (the weight of the pellets was 2.93 g) was far less than that at 1.8 V, as indicated by the current−time plot in Figure 1c. Only the residual current was recorded when the cell voltage was lowered to 1.2 V, implying no reaction undergoing at the electrodes.

The products of electrolysis at 3.2−2.0 V were black in color. At 1.8 V, the product was dark blue. Below 1.6 V, the obtained powders were nonuniform, including both white and dark colored particles. The colors of the products are believed to have originated from the Ti(III) metal centers and also the lithium content-dependent electronic structures in the compounds. Furthermore, based on the weight of the obtained product after thorough washing with water in air or acetone in an argon-filled glovebox and drying, and the total charge passed during electrolysis, including that from the background current, the current efficiency of both reactions 1 and 2 was found to be over 80%, and often to 95%. The high speed and efficiency of the electrolithiation process might have benefited from the use of the fine oxide powder with submicrometer particles, and of the relatively high electrolysis temperature (700 °C). Like most solid-phase diffusion processes, lithium intercalation proceeds to completion at a rate that increases exponentially with temperature and in a time inversely proportional to the intercalation distance.

Another point to mention is that no difference was visible between the electrolytic products washed with water in air and with acetone under argon. As will be shown later, the XRD spectra of samples washed in water and acetone are almost identical (see Figures 3 and 4), indicating the products are structurally highly stable. However, lithium loss in samples washed in water was confirmed by ICP analysis. Table 1 presents typical Li-to-Ti ratios in differently washed samples, further confirming the products obtained at 3.2 and 1.8 V to be $LiTiO_2$ and $LiTi_2O_4$, respectively. There is a small but noticeable difference in the atomic ratio of Li and Ti between the products washed with commercial (A) and dry acetone (C), implying the effect from the trace amount of water in the commercial acetone. The water influence is confirmed by the further lithium loss in samples washed in the commercial acetone followed by overnight immersion in water (B). It is well known that lithium insertion compounds synthesized, for example, by using lithium metal or an organic lithium compound are unstable in aqueous environments.[3,22,23] The presence of the Ti(III) state in the insertion compounds may be partially responsible for the low stability. However, it is also well known that the Magnelli phases[35] or the Ebonex materials[36] (TiO_{2-x}, $0 < x < 1$) contain the Ti(III) state but are still very stable in various aqueous environments. Therefore, the water−lithium ion interaction must have also played an important role in the observed lithium loss. It is interesting to note that the samples treated by overnight immersion in water still retained most of the lithium (see Table 1), indicating a partition equilibrium determined by the activities of lithium ion in the oxide and water phases. This understanding is in accordance with the XRD analyses of samples washed in water and acetone (see Figures 3 and 4) and can be compared to the literature report that hydrous Li−Ti−O compounds, for example, $Li_{0.665}Ti_{0.83}O_2 \cdot 0.2H_2O$, have been prepared

(35) *Binary Alloy Phase Diagrams*; Massalski, H., Ed.; ASM International; The Materials Information Society: U.S., 1990; Vol. 3, p 2926.

(36) Smith, J. R.; Walsh, F. C.; Clarke, R. L. *J. Appl. Electrochem.* **1998**, *28*, 1021.

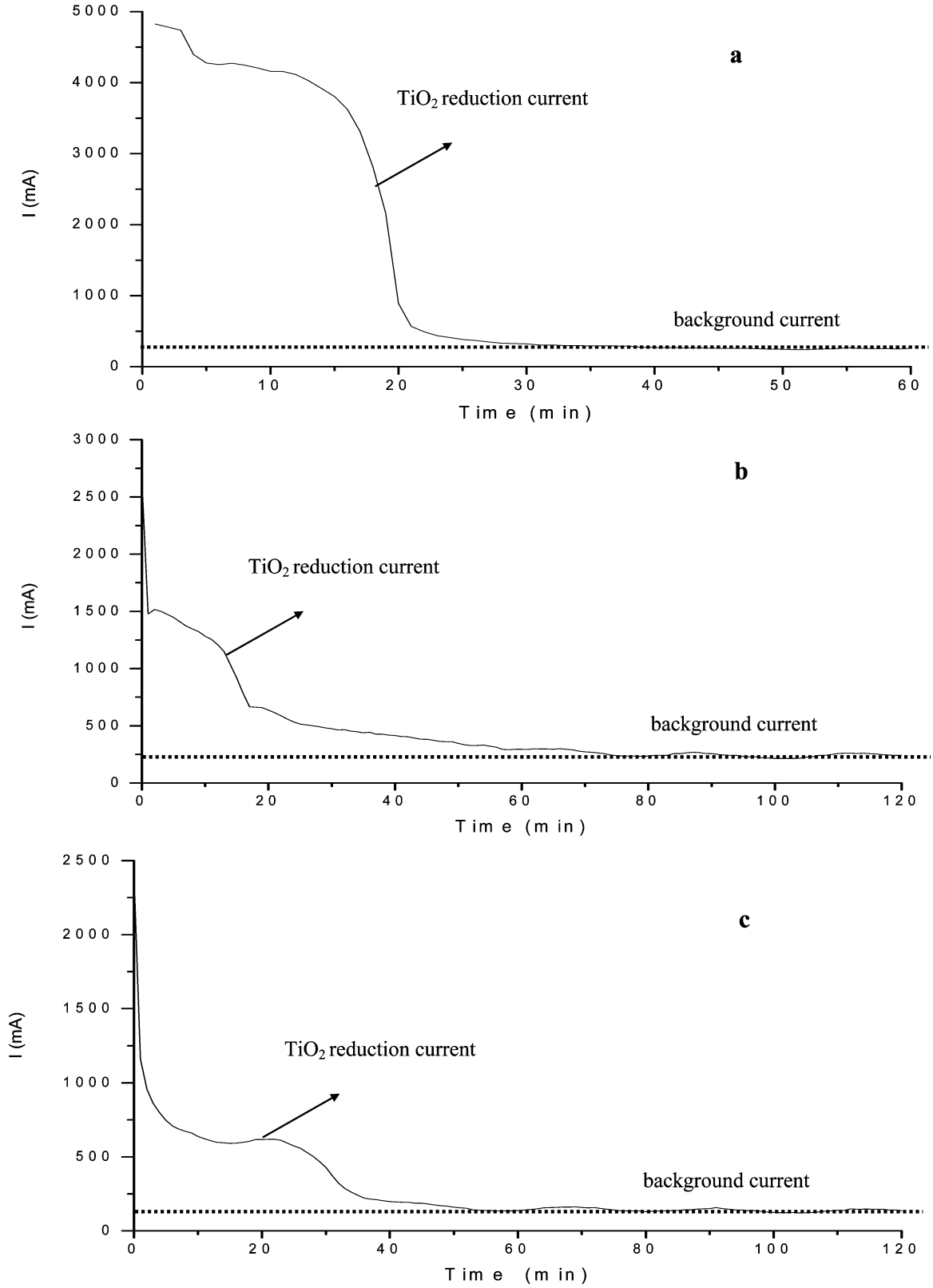

Figure 1. Current−time plots recorded during electrolysis of solid TiO_2 in molten LiCl at 700 °C with the applied voltage of (a) 3.2, (b) 1.8, or (c) 1.6 V. The horizontal dotted lines are used for subtracting the background current.

by the hydrothermal process and the structurally bound water is removable by heating to temperatures higher than 250 °C.[31]

3.2. Cyclic Voltammetry. The TiO_2 pellets used for electrolysis were too large for cyclic voltammetry. To investigate the electrochemical lithiation of TiO_2, a "TiO_2 powder modified molybdenum electrode" was fabricated (see the Experimental Section for details) and used as the working electrode. Figure 2 presents different cyclic voltammograms (CVs) measured in molten LiCl at 700 °C. The dashed line was recorded on an unmodified molybdenum wire, showing lithium deposition at about −2.10 V (vs Pt). The solid line was from the TiO_2 powder modified molybdenum electrode. There

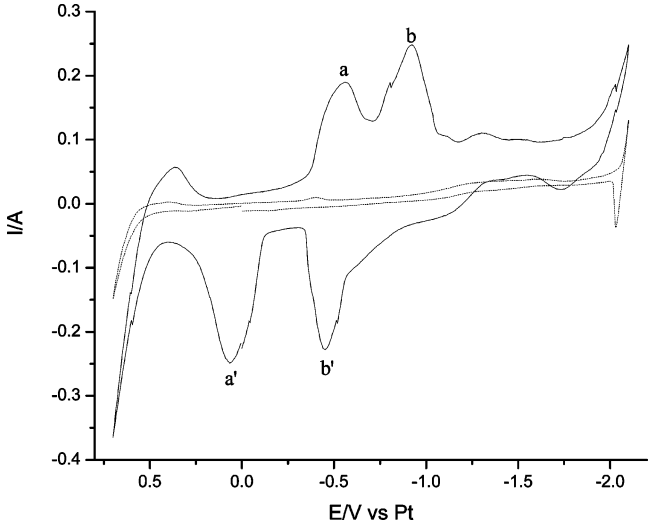

Figure 2. Cyclic voltammograms of the molybdenum wire electrode with (solid line) and without (dashed line) TiO_2 modification in molten LiCl at 700 °C. Scan rate: 0.1 V/s.

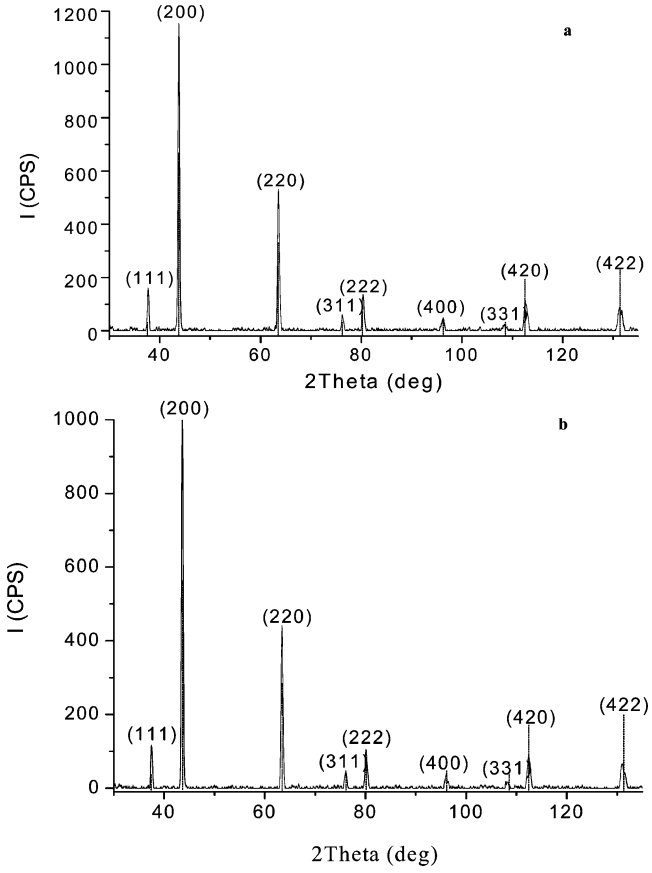

Figure 3. XRD spectra (solid lines) of the products from electrolysis at 3.2 V washed in water (a) and dry acetone (b), and those of the standard $LiTiO_2$ (dashed line).

are two couples of reduction and reoxidation peaks (**a**/**a**′ and **b**/**b**′), apparently resulting from Li^+ insertion and expulsion. The two peak couples indicate possibly two main steps of Li^+ insertion into TiO_2. The first step (peak **a**) takes place at a potential ($E_{pc/2}$) of about −0.50 V vs Pt or 1.60 V vs Li^+/Li. In this work, the decomposition voltage of LiCl was measured to be about 3.35 V at 700 °C. Therefore, it can be derived that the cell voltage is about 1.75 V for a two-electrode cell to have the cathodic reaction of peak **a** and the anodic reaction of

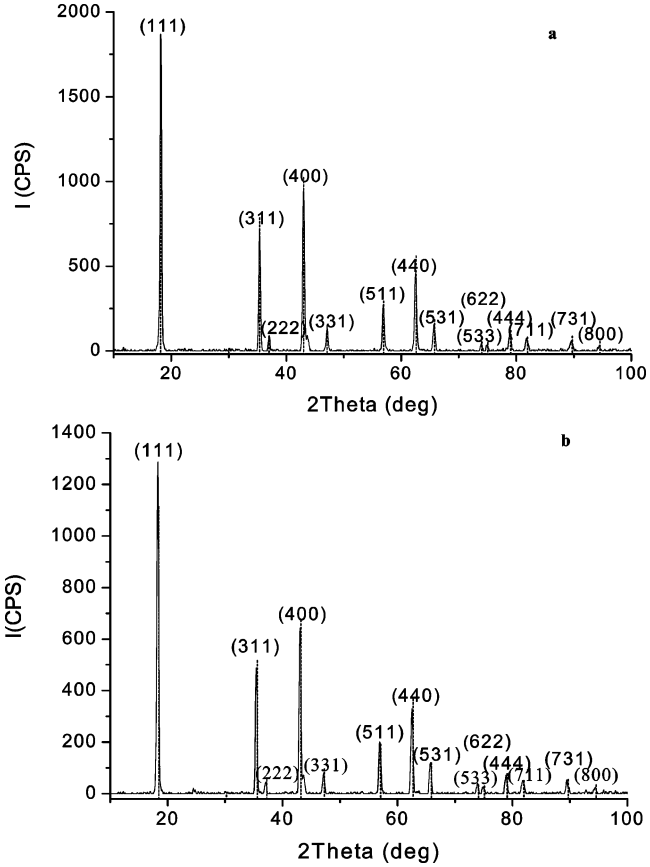

Figure 4. XRD spectra (solid lines) of the products from electrolysis at 1.8 V washed in water (a) and acetone (b), and those of the standard $LiTi_2O_4$ (dashed line).

Table 1. Results of the ICP-EAS Analysis of the Electrolytic Li−Ti−O Compounds Washed Following Different Procedures (Error: ±5%)

voltage of electrolysis	atomic ratio of Li and Ti		
	A[a]	B[b]	C[c]
1.8 V	0.44	0.36	0.54
3.2 V	0.90	0.83	0.97

[a] A: The samples were washed with as-received commercial acetone. [b] B: The samples were washed with the commercial acetone, followed by immersion in water overnight with occasional stirring. [c] C: The samples were washed in dry acetone obtained by reacting the commercial acetone with anhydrous K_2CO_3 and distillation.

chlorine evolution. The second step (peak **b**) takes place at the potential ($E_{pc/2}$) of about −0.70 V vs Pt or 1.4 V vs Li^+/Li, which corresponds to a cell voltage of 1.95 V with the product being that of the reaction of peak **b** at the cathode and chlorine gas at the anode. These derived cell voltages agree very well with the applied cell voltages of 1.8 and 2.0 V that led to reactions 2 and 1, respectively, as discussed previously. Consequently, the reactions of peaks **a** and **b** can be expressed as follows.

$$\text{peak } \mathbf{a}\text{: } 2TiO_2 + Li^+ + e \rightarrow LiTi_2O_4 \qquad (2)$$

$$\text{peak } \mathbf{b}\text{: } LiTi_2O_4 + Li^+ + e \rightarrow 2LiTiO_2 \qquad (3)$$

Changing the potential window limits confirmed that the reverses of reactions 2 and 3 correspond to peaks **a**′ and **b**′, respectively.

3.3. X-ray Diffraction Analyses. X-ray diffraction (XRD) was used to confirm the structure of the starting

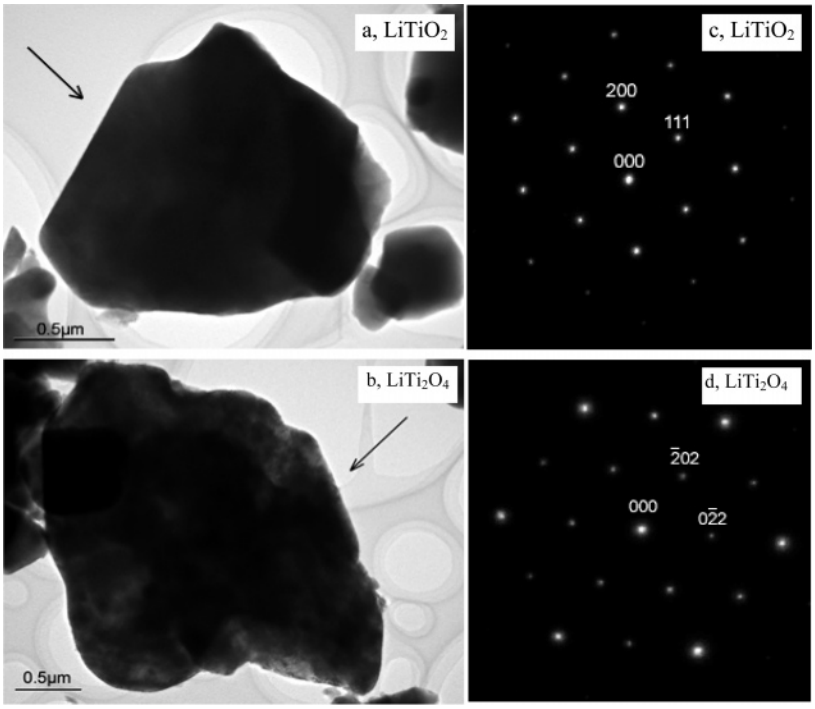

Figure 5. Bright field TEM images of particles of electrochemically prepared (a) $LiTiO_2$ and (b) $LiTi_2O_4$, and their electron diffraction patterns in the $0\bar{1}1$ zone and 111 zone, (c) and (d), respectively, from the particles indicated by the arrows.

materials and the products of electrolysis. The analysis demonstrated that the sintered TiO_2 was dominated by the anatase form. Figure 3a and b displays the XRD spectra of the products obtained from electrolysis at 3.2 V and washed in water and dry acetone, respectively. These spectra match very well with that of the rock salt-type $LiTiO_2$ standard (JCPDS No.16-0223) for the main peaks. In addition, the sharp and narrow shapes of the peaks and the absence of noticeable impurity signals greater than the background noises are proof of the product being highly crystalline and very pure. The spectra of the samples from electrolysis at 2.8, 2.4, and 2.0 V are almost identical to that in Figure 3a. These results are in agreement with reaction 1. The XRD spectra are presented in Figure 4a and 4b of the products from electrolysis at 1.8 V and washed in water and dry acetone, respectively. Again, the patterns of these spectra are the same as that of the spinel-type $LiTi_2O_4$ (JCPDS No.40-0407) and hence support reaction 2. The product from electrolysis at 1.6 V showed that the main phase in the product was TiO_2, but the $LiTi_2O_4$ phase, although in a small amount, was observed as well. Electrolysis at 1.2 V did not change the phase in the TiO_2 cathode because the XRD spectrum of the product was identical to that of TiO_2.

3.4. Transmission Electron Microscopy. Figure 5a and b demonstrates two representative bright field TEM images of the electrochemically prepared $LiTiO_2$ and $LiTi_2O_4$ samples, respectively. The electron diffraction pattern of a $LiTiO_2$ particle in the $0\bar{1}1$ zone is presented in Figure 5c. It proves the particle is a single crystal with the rock salt structure and further confirms that the prepared $LiTiO_2$ was in a single phase as indicated by the XRD data in Figure 3. The electron diffraction pattern of a $LiTi_2O_4$ particle in the 111 zone is shown in Figure 5d, showing the characteristics of the spinel structure, which matches quite well the XRD patterns in Figure 4.

4. Conclusions

This report demonstrates, for the first time, the production of the rock salt-type $LiTiO_2$ and spinel-type $LiTi_2O_4$ in single phase by electrolysis of solid TiO_2 in a molten salt. Cyclic voltammetry of a TiO_2 modified molybdenum electrode in molten LiCl suggests two steps of electrochemical Li^+ insertion into solid TiO_2 at different potentials. The charge−mass correlation obtained from constant voltage electrolysis indicates the formation of $LiTiO_2$ in the range of 2.0−3.2 V and of $LiTi_2O_4$ at about 1.8 V. Inductively coupled plasma, X-ray diffraction, and transmission electron microscopy analyses further confirm the formation of the two stoichiometric compounds and also show that the products are in high purity and crystallinity and can structurally withstand water washing. The current efficiency is above 80% and reaching 95%, promising a simple, fast, and controllable electrochemical synthesis route for future commercial application. We anticipate that the electrochemical method reported in this paper is potentially applicable for the lithiation of other transition metal oxides.

Acknowledgment. We would like to thank the Ministry of Education of China and the Natural Science Foundation of China (Grant No. 20125308) for financial support.

CM0494148